ASSESSMENT OF HYDROACOUSTIC PROPAGATION USING AUTONOMOUS HYDROPHONES IN THE SCOTIA SEA

Haru Matsumoto[1], Del R. Bohnenstiehl[2], Robert P. Dziak[1], Robert W. Embley[3], and Minkyu Park[4]

Cooperative Institute for Marine Resources Studies[1], North Carolina State University[2], Pacific Marine Environmental Laboratory, National Oceanic Administration[3], and Korea Polar Research Institute[4]

Sponsored by the National Nuclear Security Administration

Award No. DE-AI52-08NA28654
Proposal No. BAA08-36

ABSTRACT

The remote area of the Atlantic Ocean near the Antarctic Peninsula and the South Scotia Sea is a region where acoustic surveillance by International Monitoring System hydrophones is at best limited. Sound originating in this area is either blocked or hindered by the South Georgia, South Sandwich Islands and the associated seafloor ridge system, making the region a potential hydroacoustic blind spot. To investigate the sound propagation and interferences affected by these landmasses in the vicinity of the Antarctic polar front, an array of autonomous hydrophones (AUHs) was deployed in the Scotia Sea in December 2007. In January 2009, five AUHs were recovered, completing a 13-month-long acoustic monitoring operation. Four of the recovered instruments continuously recorded low-frequency acoustic signals (1–110 Hz) at a sampling rate of 250 Hz, with one instrument sampling at a rate a rate of 1000 Hz (1–440 Hz band-passed). The submerged moorings utilized autonomous crystal oscillator clocks, with small time shifts that average ~2 seconds per year. Despite the fact that the high-latitude ocean lacks a deep sound channel, low-frequency sound tends to travel relatively efficiently. Regional seismo-acoustic signals (bottom sources) and episodic tremors from large icebergs (near-surface sources) were utilized as natural sound sources. Surface sound sources, e.g., ice-related events, tend to suffer less transmission loss (TL) and dominate the background noise as a result of surface duct transmission and less interaction with seafloor features. On the other hand, earthquake-generated signals (bottom sources) interact more strongly with the shallow arc, and TL tends to be larger. The RAM PE-code (Collins, 1993a,b) was used to model TL, and the AUH data were used to compare with these modeling results. Both the observational and model results indicate a unique acoustic environment of the Scotia Sea, including the evidences of reflected T-waves by the steep slope of the South Georgia Island and efficient P-to-T conversion by the Scotia Ridge system. We found that transmission loss for the shallow-depth sources tends to follow a ~17log10(r) loss model at ranges of 10s to100s km. Seafloor sources are characterized by greater TL, and where the range-dependent bathymetry shallows, the results deviate strongly from a simple $\log_{10}(r)$ relationship. We present two-dimensional path-dependent TL models relative to the hydrophone receivers for near-surface and bottom sources.

OBJECTIVES

The International Monitoring System (IMS) includes a sparse network of sound-channel-moored hydrophones and island-based seismic stations deployed in an effort to monitor the global oceans for signs of explosive tests that may be conducted below or just above the sea surface. Relative to the IMS sites, the most remote portions of the global ocean lie at high polar latitudes. Such settings are unique in that acoustic propagation conditions become surface limited as the deep-ocean sound-channel disappears in response to the nearly isothermal temperature structure of the polar oceans. Moreover, these areas are characterized by high seasonal variability in the background noise field, due in part to the retreat and advance of sea ice and the movement and breakup of drifting icebergs.

This study investigates the acoustic environment at high southern latitudes (~50°–60°) within the Scotia Sea—an area of the southern ocean surrounded by Tierra del Fuego; the Falkland Islands; the South Georgia, South Sandwich, and South Orkney Islands; and the Antarctic Peninsula. It is a tectonic and volcanically active area, providing an abundance of sub-seafloor earthquake sources (T-waves) that produce acoustic energy dominantly in the 5- to 35-Hz band. The surface waters also host a number of drifting icebergs that produce broadband energy with frequencies extending above 125 Hz, with the southern-most hydrophones under sea ice cover during the height of the Austral winter (Matsumoto et al., 2009).

Both earthquake- and ice-generated sound sources within the Scotia Sea were recorded using a network of five autonomous underwater hydrophones (AUHs) (Fox et al., 2001), deployed for a period of ~13 months beginning in December of 2007. The hydrophones recorded continuously with four instruments sampling at 250 Hz (1–110 Hz band passed) and one instrument sampling at a rate of 1000 Hz (1-440 Hz band passed). The submerged instrumentation used autonomous crystal oscillators clocks, with small time shifts that averaging ~2 seconds per year. To avoid the largest of the drifting ice masses in the southern ocean, the AUHs were floated ~500 m below the sea surface. Figure 1 shows a schematic of the polar AUH mooring design.

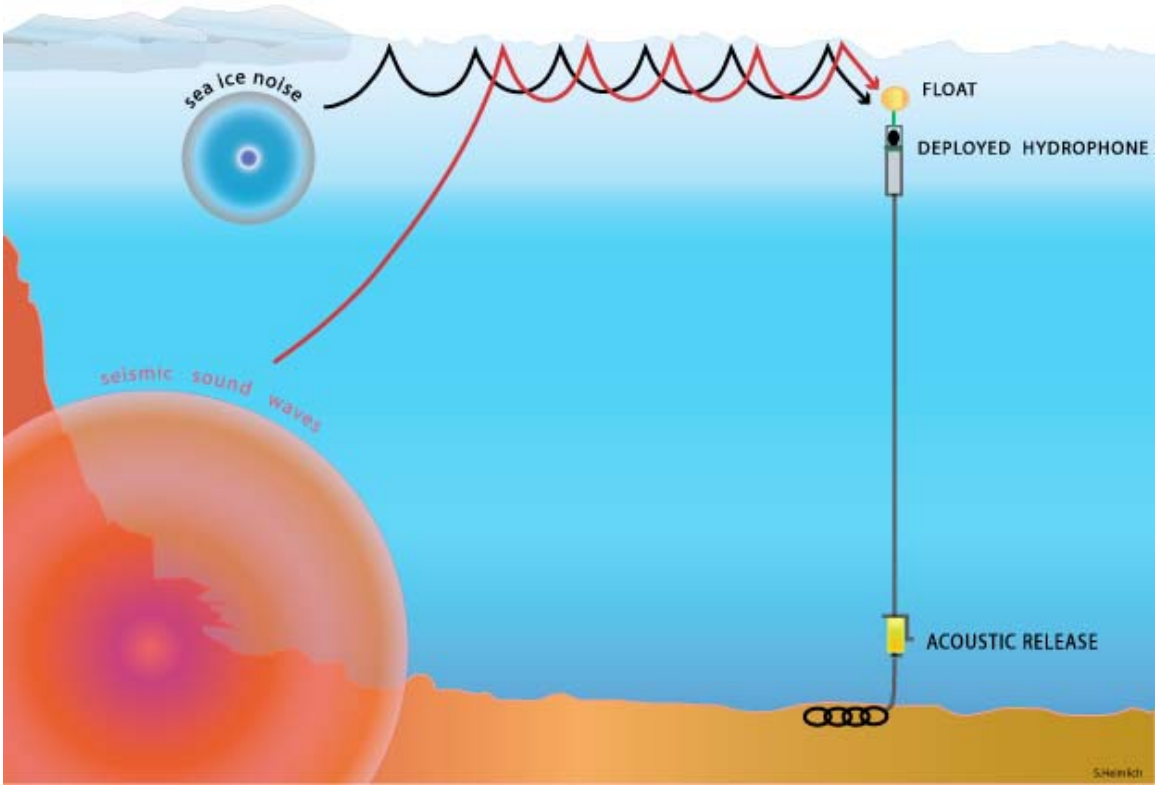

Figure 1. Schematic of high-latitude autonomous hydrophone mooring.

RESEARCH ACCOMPLISHED

Propagation Modeling

Path-dependant TL was modeled using a range-dependent implementation of the RAM PE-code (Collins, 1993a,b). Modeling incorporated the latest global ocean bathymetric data (1 arc-minute resolution) (Amante and Eakins, 2009), annually averaged oceanographic information taken from the 2005 version of the Word Ocean Atlas (WOA-05) (National Oceanographic Data Center, 2008) and National Oceanic and Atmospheric Administration's (NOAA's) 2-arc-minute sediment thickness model (Divins, 2009). The bathymetry and sediment thickness within the Scotia Sea area are shown in Figures 2 and 3. Bathymetry and sediment accumulation patterns primarily reflect the structure of the Scotia subduction zone and volcanic arc.

Model sound sources were located on a ~10 by 10 km grid of points spanning the acoustic environment between 53° and 63° S latitude and 15° and 45° W longitude. Two source depths were considered: (a) 100 m (fixed), simulating the propagation of acoustic energy from a drifting ice mass or an explosion at or near the sea surface, and (b) near sea bottom, where the depth of the source is prescribed based on the local depth at each grid node ($Z^{source} = Z^{bath} + \Delta Z^{model}$). For each source location, the bathymetry and range-dependent sound velocity information were extracted for the relevant databases. Transmission loss was then calculated for each grid relative to the receiver and stored in a matrix. For the models shown here, the source frequency was set at 15 Hz. Signal blockage was assumed if the water depth dropped below ¼ of the acoustic wavelength at any point along the propagation path.

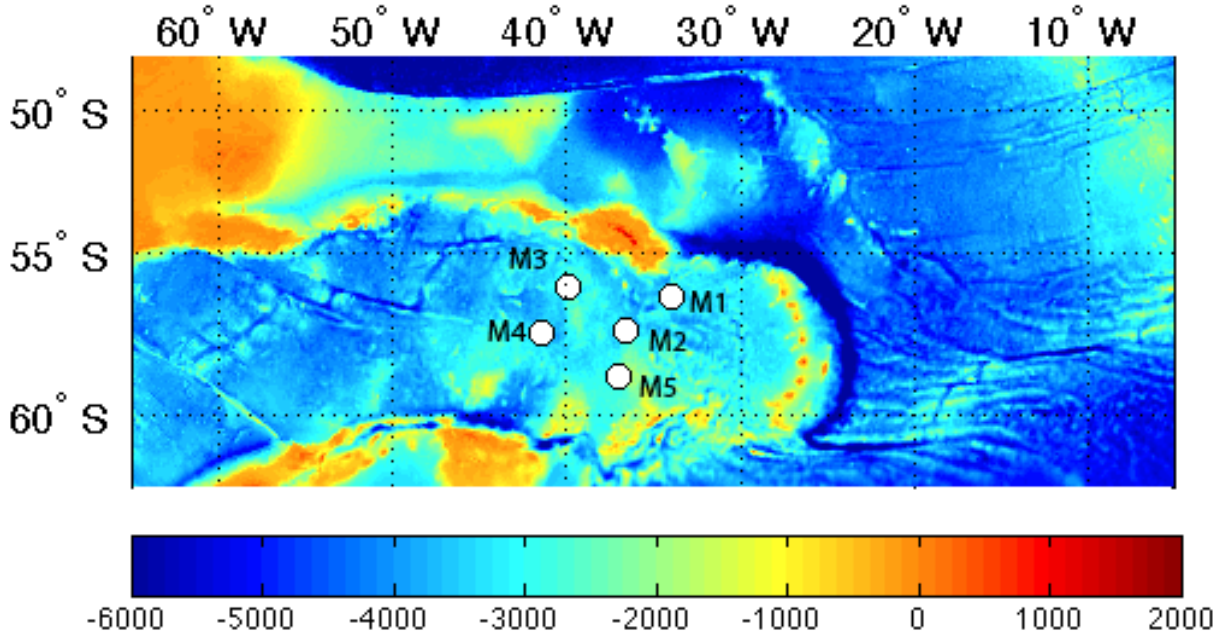

Figure 2. Bathymetry of the Scotia Sea with hydrophones (white circles) labeled M1–M5. Station M1 is sampled at 1000 Hz and the remaining stations at 250 Hz. Depths are displayed in meters. Data are from the ETOPO 1 database (Amante and Eakins, 2009). The amount of ship-based multibeam data is extremely limited in the region.

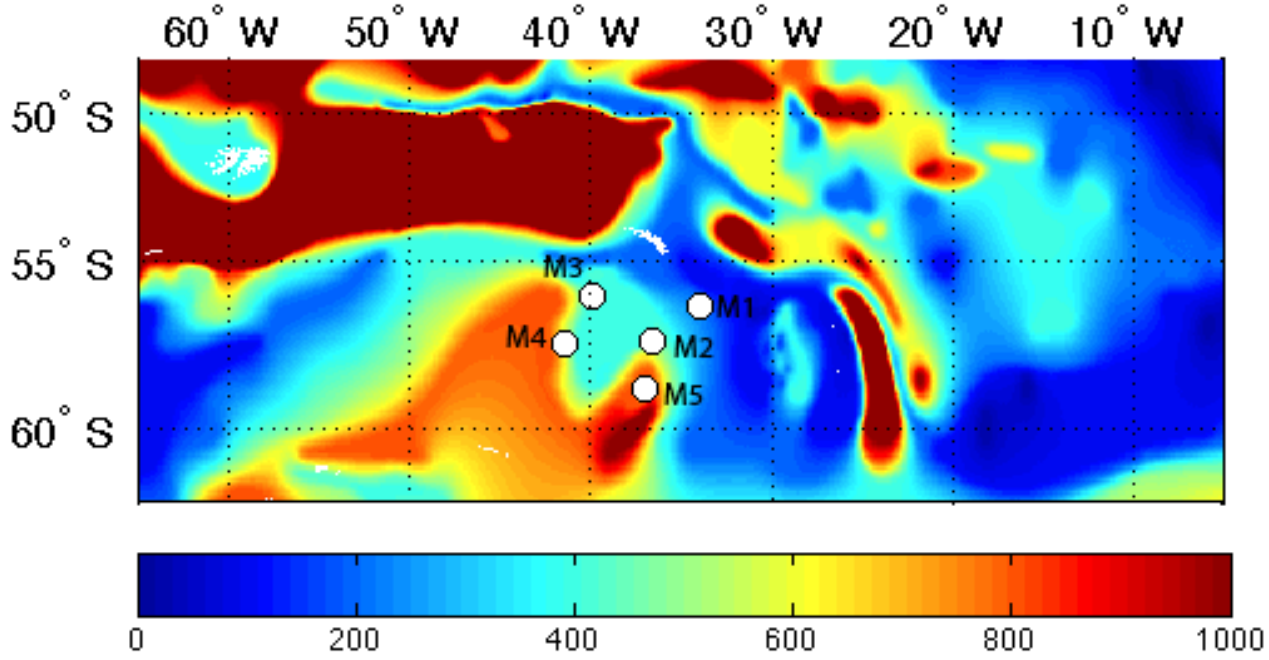

Figure 3. Scotia Sea sediment thicknesses are displayed in meters. Data are from the NOAA sediment thickness compilation (Divins, 2009).

The results of this approach are demonstrated in Figure 4 for station M3. The principal observation that can be made is the difference in TL for the bottom (Figure 4a) and near-surface (Figure 4b) source depths considered. Due to the surface reflected-refracted propagation style, the Scotia Volcanic Arc and the ridges that bound the Scotia Plate to the north and south minimally affect shallow surface-duct sources. Near-bottom earthquake sources, however, interact more strongly with the shallow arc, and TLs are higher as a result.

Matsumoto et al. (2009) previously described a set of double-peaked T-waves representing shallow earthquakes generated to the east of the Scotia Arc. According to their model, the early-arriving phase represents acoustic energy converted between the event epicenter and the station, along the shallow west-facing slope of the volcanic arc. For the bottom source-depth model (Figure 4a), a band of low TL can be seen, indicating the relatively efficient propagation of this signal through down-slope conversion.

Figure 5a examines the TL versus range data for propagation to station M3, with several standard transmission loss models shown for reference. For the ranges investigated here (10-100's km), shallow source depth TL is approximated by a ~17log10(r) model. A pair-wise comparison (Figure 5b) of the shallow and bottom source depth models shows that earthquake sources undergo greater TL at all ranges and these differences increase for paths that cross the Scotia Arc (ranges > 500-600 km). Model results for the other stations show similar patterns.

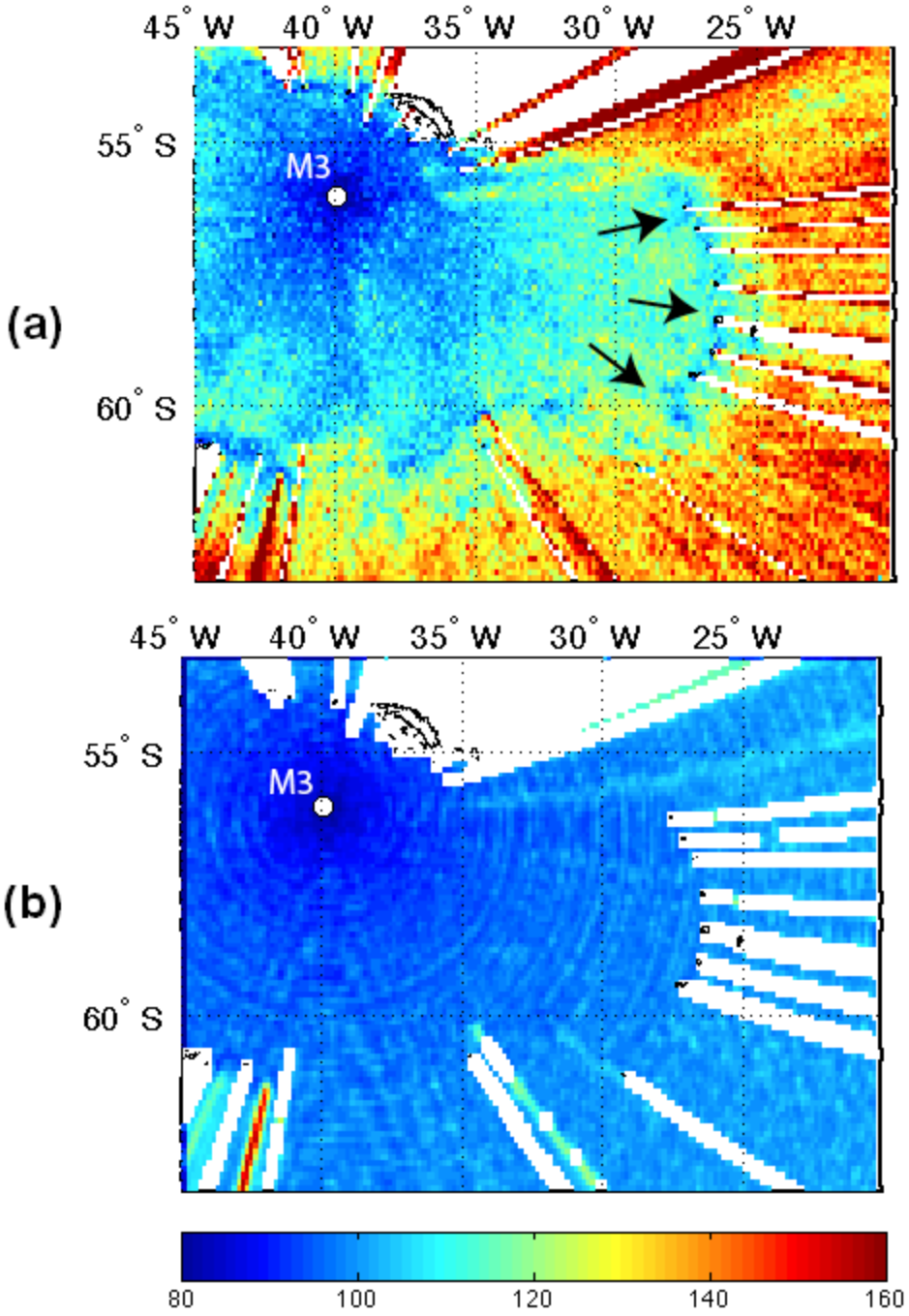

Figure 4. Path-dependent TL model (dB re 1uPa) for (a) bottom and (b) fixed 100-m source depths. Black arrows in (a) highlight the zone of slope conversion along the westward-facing arc.

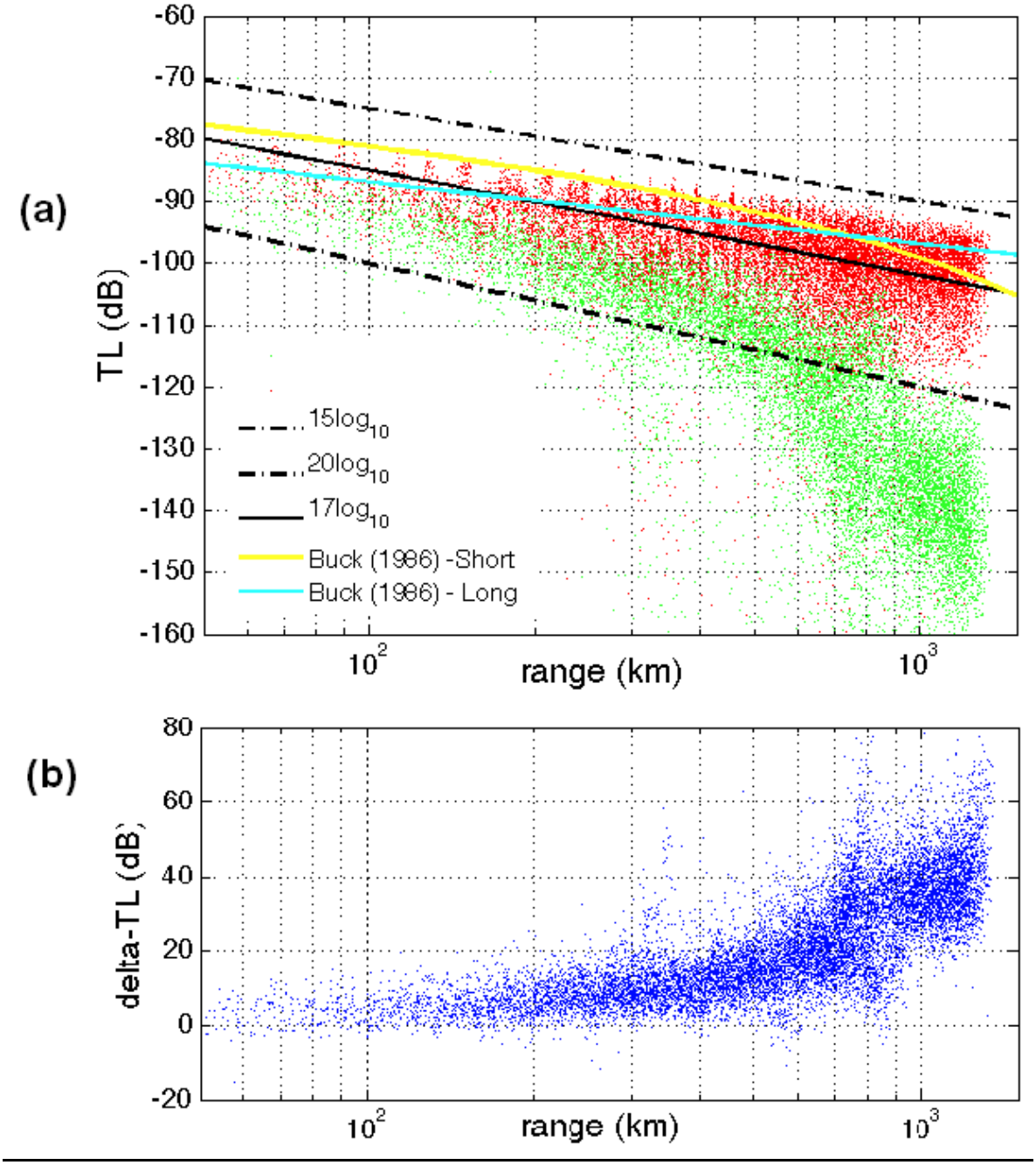

Figure 5. (a) TL versus range with the model domain shown in Figure 4 for station M3 (15 Hz). Red dots are TLs of ice-related surface origin; green dots are of seismic bottom sources. Black lines show reference TL models of 10, 17, and 20*log10(r); yellow and light blue lines show the Arctic propagation model of Buck (1986) at short and long ranges (assume zero ice roughness). (b) TL differences for near-bottom and 100-m depth sources throughout the model domain.

CONCLUSIONS AND RECOMMENDATIONS

Within the Scotia Sea, TL for the shallow-depth sources tends to follow a ~17log10(r) loss model at ranges of 10s to100s km. Near-bottom source depths are characterized by greater TL, and where the range-dependent bathymetry shallows, the results may deviate strongly from a simple $\log_{10}(r)$ relationship. The results demonstrate that the efficiency of acoustic propagation may be strongly source-depth dependant a high latitudes. It also indicates that in the polar region, if a traditional cylindrical-law loss model is applied for the near surface-events, the transmission loss is too small, and as a result yield estimates may be too low.

Traditional line-of-sight blockage maps do not account for this source-depth dependence. Moreover, our model results indicate that empirical blockage maps, which may largely or partially rely on sea-bottom earthquake sources, will tend to over-estimate blockage for high-latitude areas with significant topography. Path-specific TL models overcome these limitations and can be used to improve blockage calculations, validate specific TL versus range relationships, and provide better estimates of T- and H-phase source levels.

ACKOWLEDGEMENTS

We would like to express our gratitude to Dr. Chris Hindley and Dr. Anthony Martin of British Antarctic Survey for carrying out the deployment of M6 in the international waters on the north side of South Georgia Island. We also thank the officers and crew of the *R/V Yuzhmorgeologiya* and *M/V Pharos SG* for deploying and recovering the hydrophones under unfavorable weather conditions. We are also indebted to the base commander Mr. Richard McKee on the Falkland Islands for help coordinating the hydrophone recovery operation. Iceberg position and sea ice extent were provided by the courtesy of Center for Remote Sensing at Brigham Young University. Finally we express our deep gratitude to the Korea Polar Research Institute for providing the ship time and logistic support at the King Sejong Antarctic base.

REFERENCES

Amante, C. and B. W. Eakins (2009). ETOPO1 1 Arc-Minute Global Relief Model: Procedures, Data Sources and Analysis. NOAA technical memorandum NESDIS NGDC-24.

Buck, B. M. (1986), Long term statistical measurements of environmental acoustic parameters in the Arctic, *AEAS Report No. 2—Low Frequency Transmission Loss Measurements in the Central Arctic Ocean*, Polar Research Lab, TR-55.

Collins, M. D. (1993a). A split-step Padé solution for the parabolic equation method, *J. Acoust. Soc. Am*., 93: 1736–1742.

Collins, M. D. (1993b). An energy-conserving parabolic equation for elastic media, *J. Acoust. Soc. Am*., 94: 975–982.

Divins, D. L. (retrieved 2009). NGDC Total Sediment Thickness of the World's Oceans & Marginal Seas, http://www.ngdc.noaa.gov/mgg/sedthick/sedthick.html

Fox, C. G., H. Matsumoto, and T-K. A. Lau (2001). Monitoring Pacific Ocean seismicity from an autonomous hydrophone array, *J. Geophys. Res*., 106: 4183–4206.

Matsumoto, H., D. Bohnenstiehl, R. Dziak, M. Park, and M. Fowler (2009). Hydroacoustic Monitoring of the Scotia Sea: Autonomous Hydrophone Experiment, in *Proceedings of the 2009 Monitoring Research Review: Ground-Based Nuclear Explosion Monitoring Technologies*, LA-UR-09-05276, Vol. 1, pp. 605–612.

National Oceanographic Data Center (retrieved 2008). World Ocean Atlas 2005, http://www.nodc.noaa.gov/OC5/WOA05/pr_woa05.html